Nimbus-5 ESMR Polar Gridded Brightness Temperatures, Version 2

USER GUIDE

How to Cite These Data

As a condition of using these data, you must include a citation:

Parkinson, C. L., J. C. Comiso, and H. J. Zwally. 1999. *Nimbus-5 ESMR Polar Gridded Brightness Temperatures, Version 2.* [Indicate subset used]. Boulder, Colorado USA. NASA National Snow and Ice Data Center Distributed Active Archive Center. https://doi.org/10.5067/CIRAYZROIYF9. [Date Accessed].

FOR QUESTIONS ABOUT THESE DATA, CONTACT NSIDC@NSIDC.ORG

FOR CURRENT INFORMATION, VISIT https://nsidc.org/data/NSIDC-0077

National Snow and Ice Data Center

TABLE OF CONTENTS

1 DETAILED DATA DESCRIPTION

1.1 Format

Data are stored in 2-byte integer flat-binary arrays. The size of the arrays are 304 columns x 448 rows for the north polar region and 316 columns x 332 rows for the south polar region. Data are stored as compressed daily files.

1.2 File Naming Convention

Adjusted brightness temperatures: `ESMR_AdjustedTB_h_yyyyddd.bin`

Where:

`h` = hemisphere (`N` or `S`)
`yyyy` = 4-digit year
`ddd` = 3-digit day of year

1.3 File Size

Northern files are 272.384 KB uncompressed.
Southern files are 209.824 KB uncompressed.

1.4 Usage

Users wishing to create custom sea ice concentrations should refer to the Appendix in the user guide for Nimbus-5 ESMR Polar Gridded Sea Ice Concentrations, Version 1, which describes the calculations required. Please note, however, that it may be difficult to compare these sea ice concentrations with the SMMR and SSM/I sea ice concentrations, because no overlap period exists between the SMMR and ESMR instruments. Additionally, because ESMR has just one channel of data, the sea ice concentrations derived from ESMR may not be as accurate as those derived from the SMMR and SSM/I instruments.

1.5 Spatial Coverage

Instrument coverage is global except for circular sectors centered over the pole, 280 km in radius, located poleward of 87°N and 87°S, which are never measured due to orbit inclination. Data set coverage includes the polar regions defined by the spatial coverage maps. Refer to Figures 1 and 2.

1.6 Spatial Coverage Map

ESMR data are gridded to the SSM/I polar stereographic grids.

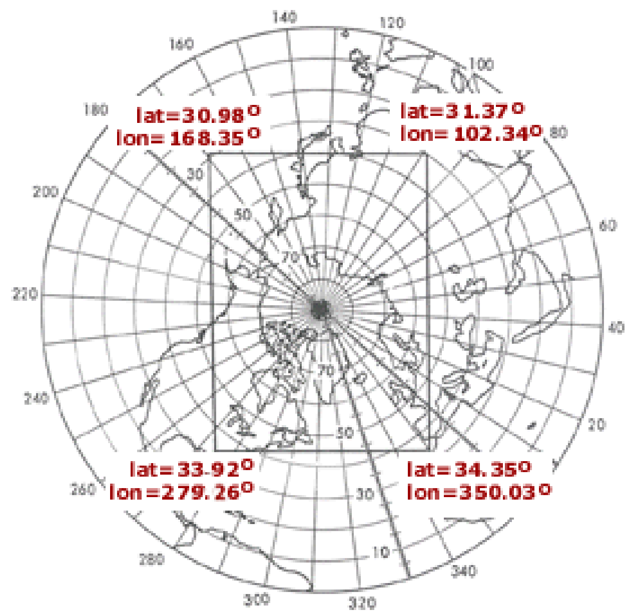

Figure 1. Northern Hemisphere

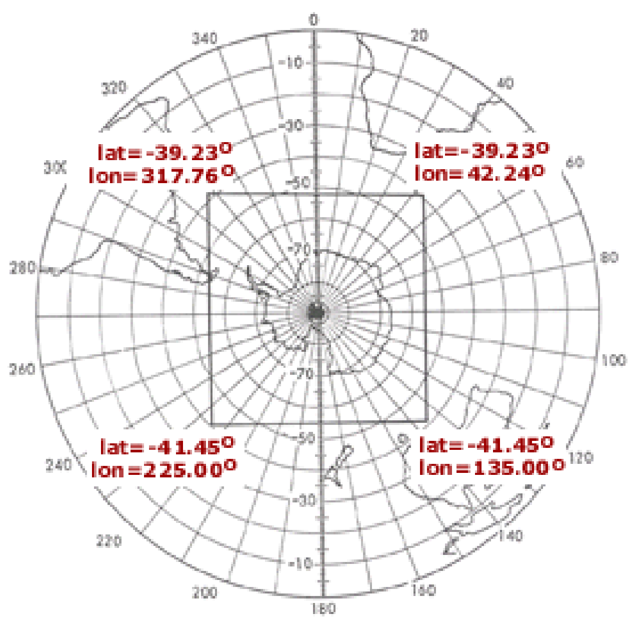

Figure 2. Southern Hemisphere

1.6.1 Spatial Resolution

The ESMR footprint size varies from approximately 32 km x 32 km to about 28 km x 28 km at 50° latitude. Gridded resolution is 25 km.

1.6.2 Projection

ESMR brightness temperature grids are in a polar stereographic projection, which specifies a projection plane (i.e., the grid) tangent to the earth at 70°. The planar grid is designed so that the grid cells at 70° latitude are 6.25 km x 6.25 km. For more information on this topic please refer to Pearson (1990) and Snyder (1987).

The polar stereographic projection often assumes that the plane (grid) is tangent to the Earth at the pole. Thus, there is a one-to-one mapping between the Earth's surface and grid (with no distortion) at the pole. Distortion in the grid increases as the latitude decreases because more of the Earth's surface falls into any given grid cell, which can be quite significant at the edge of the northern polar grid where distortion reaches 31%. The southern polar grid has a maximum distortion of 22%. To minimize the distortion, the projection is true at 70° rather than the poles. This increases the distortion at the poles by three percent and decreases the distortion at the grid boundaries by the same amount. The latitude of 70° was selected so that little or no distortion would occur in the marginal ice zone. Another result of this assumption is that fewer grid cells will be required as the Earth's surface is more accurately represented.

The polar stereographic formulae for converting between latitude/longitude and X-Y grid coordinates are taken from Snyder (1982). This projection assumes a Hughes ellipsoid with a radius of 3443.992 nautical mi or 6378.273 km and an eccentricity (e) of 0.081816153 (or e**2 = 0.006693883).

1.6.3 Grid Description

North: 304 columns, 448 rows
South: 316 columns, 332 rows

SSM/I Polar Stereographic Grid Coordinates

The origin of each x, y grid is the pole. The grids' approximate outer boundaries are defined in Tables 1 and 2. Corner points are listed; apply values to the polar grids reading clockwise from upper left. Interim rows define boundary midpoints.

Table 1. North Polar Grid Description

X(km)	Y(km)	Latitude (deg)	Longitude (deg)	
-3850	5850	30.98	168.35	corner
0	5850	39.43	135.00	midpoint
3750	5850	31.37	102.34	corner
3750	0	56.35	45.00	midpoint
3750	-5350	34.35	350.03	corner
0	-5350	43.28	315.00	midpoint
-3850	-5350	33.92	279.26	corner
-3850	0	55.50	225.00	midpoint

Table 2. South Polar Grid Description

X(km)	Y(km)	Latitude (deg)	Longitude (deg)	
-3950	4350	-39.23	317.76	corner
0	4350	-51.32	0.00	midpoint
3950	4350	-39.23	42.24	corner
3950	0	-54.66	90.00	midpoint
3950	-3950	-41.45	135.00	corner
0	-3950	-54.66	180.00	midpoint
-3950	-3950	-41.45	225.00	corner
-3950	0	-54.66	270.00	midpoint

1.7 Temporal Coverage

Adjusted: 1972-12-11 to 1977-05-16

Gridded North: 1972-12-12 to 1977-05-08

Gridded South: 1972-12-12 to 1977-05-10

1.7.1 Temporal Resolution

Data consist of daily-averaged brightness temperatures, but some data are missing where adjustments could not be applied successfully. See Tables 3 and 4 for a list of missing dates.

Table 3. Missing Dates for the Northern Hemisphere

Year	Day of Year
1972	001-345
1973	060, 208, 209, 213, 232
1974	041, 042
1975	155-229, 231, 233, 235-237, 239, 241, 243, 245, 247, 249, 251, 253, 255, 257, 259, 261, 263, 267, 269, 271, 273, 275, 277, 281, 283, 285, 293, 299, 305, 307, 309, 311, 313, 315, 317, 319, 321, 323, 325, 327, 329, 331, 333, 335, 337, 339, 341, 343, 345, 347, 349, 359, 365
1976	095, 111, 145, 167, 169, 199, 201, 205, 231, 233, 235, 241, 243, 291, 293, 295, 297, 305, 321, 323, 325, 327, 329, 353, 355
1977	025, 061, 103, 109, 123, 137-365

Table 4. Missing Dates for the Southern Hemisphere

Year	Day of Year
1972	001-345
1973	060, 208, 209, 213, 232, 350
1974	041, 042
1975	155-229, 231, 233, 235 - 237, 239, 241, 243, 245, 247, 249, 251, 253, 255, 257, 259, 261, 263, 267, 269, 271, 273, 275, 279, 281, 283, 285, 293, 299, 305, 307, 309, 311, 313, 315, 317, 319, 321, 323, 325, 327, 329, 331, 333, 335, 337, 339, 341, 343, 345, 347, 349, 359, 365
1976	095, 111, 145, 167, 169, 199, 201, 205, 231, 233, 235, 291, 293, 295, 297, 305, 321, 323, 325, 327, 329, 353, 355
1977	061, 103, 109, 123, 137-365

1.8 Parameter or Variable

1.8.1 Parameter Description

Brightness Temperature: effective temperature of a blackbody radiating the same amount of energy per unit area at the same wavelength as the observed body - also called effective temperature.

Brightness temperatures are calculated at 19.35 GHz vertical and horizontal frequencies from ESMR channel output. Brightness temperature grids are precise to 1/10 Kelvin.

1.8.2 Unit of Measurement

Brightness temperatures are measured in Kelvins.

1.8.3 Parameter Source

Nimbus-5 ESMR

1.8.4 Parameter Range

Data are stored as 2-byte, binary integer arrays of brightness temperatures that range from approximately 50 K to 310 K. Missing data are indicated by the value -10.

1.8.5 Sample Data Record

See the "Additional Calibration" section for images of gridded ESMR brightness temperature data.

1.9 Error Sources

The following details are summarized from Parkinson et al. (1987). Please consult this source for a more complete description of the data adjustments.

Initial geolocation errors of up to several hundred kilometers were substantially reduced after 1975 by using ephemeris data calculated from satellite tracking parameters (all prior CBT tapes were revised to eliminate errors). Now, calculated positions appear to be accurate to within 30 km, which is the approximate resolution used in mapping the data.

In addition, many of the early brightness temperatures were contaminated by abnormal brightness temperatures. Most of the inaccurate data have been eliminated by requiring values of calibration parameters to fall within acceptable limits. Arctic data have considerably more data gaps than Antarctic data.

Since both hot-load and cold-load reference temperatures are necessary for calibrating the radiometer, the instrument was considered uncalibrated in cases where both temperatures were not recoverable. ESMR was in this mode most during March, April, May and August of 1973, and in November and December, 1976. Data obtained during these months are insufficient for generating monthly averages.

During June, July and August, 1975, the data acquisition system for Nimbus-5 was turned off because the instrument acquisition system was needed for the newly launched Nimbus 6-satellite. Data acquisition for the Nimbus-5 was restored on an every-other-day basis in September 1975.

1.10 Quality Assessment

NSIDC has not validated the ESMR data; they remain unchanged from the original GSFC format.

2 SOFTWARE AND TOOLS

2.1 Software and Tools

Because ESMR brightness temperatures are in the same polar stereographic grid as SSM/I brightness temperatures, some SSM/I tools can be used to read and display the ESMR data. Included are IDL display programs to extract and display the data, geolocation tools, and masking tools that limit the influence of non-sea ice brightness temperatures. Table 1 lists the tools that can be used with this data set. For a comprehensive list of all polar stereographic tools, see the Polar Stereographic Data Tools Web page.

Note: Due to the age of the ESMR data, land grid cells embedded within ESMR data files may not be completely consistent with the current land masks provided in Table 5. Thus, cells that are displayed as land in the ESMR data files may not be displayed as land in the newest land masks, and vice versa.

Table 5. Tools for this Data Set

Tool Type	Tool File Name(s)
Data Extraction	extract.pro
Geocoordinate	locate.for
	mapll.for and mapxy.for
	psn25lats_v3.dat and pss25lats_v3.dat
	psn25lons_v3.dat and pss25lons_v3.dat
Pixel-Area	psn25area_v3.dat and pss25area_v3.dat
Masks and Overlays	coast_25n.msk and coast_25s.msk
	gsfc_25n.msk and gsfc_25s.msk
	landmask.ntb and landmask.stb
	ltln_25n.msk and ltln_25s.msk

3 DATA ACQUISITION AND PROCESSING

3.1 Theory of Measurements

The microwave radiometer measures the emitted energy from the earth/atmosphere system in the microwave wavelength region (1-100 GHz). Since the Rayleigh-Jeans approximation holds in the microwave wavelength regime, the emitted energy is proportional to the temperature of the radiator to a first order; therefore, intensity is synonymous with temperature at these wavelengths.

Rayleigh-Jeans equation:

$E=2k_BTcv^2$

Where:

k_B = Boltzmann's constant
c = speed of light
v = wave number

3.2 Data Acquisition Methods

Telemetry data from the Nimbus-5 satellite were transmitted to two spaceflight tracking and data network stations located near Fairbanks, Alaska, and Rosman, North Carolina. The data were relayed from these stations to the NASA Goddard Space Flight Center (GSFC). At GSFC, the telemetry data were unpacked, decommutated, supplemented with flags and ends of files, and stored on magnetic tapes called Experimental Tapes (ETs). For data processing convenience, the data from the ESMR instrument were combined from several ETs to form Stacked Experimental Tapes (SETs). The 10-bit telemetry data on the ETs were converted to 32-bit format on the SETs for use on the GSFC computers. The SETs were used with ephemeris tapes to generate Earth-located Calibrated Brightness Temperature (CBT) tapes.

3.3 Source or Platform Collection Environment

The Nimbus-5 flew in a circular sun-synchronous orbit at 1112 km (600 nautical miles), had a local noon (ascending) and midnight (descending) equator crossing, and an 81° retrograde inclination. Successive orbits crossed the equator at 27° longitude separation. The orbital period was about 107 minutes. Nimbus-5 used an attitude control system which stabilized the spacecraft with respect to the earth and orbital plane, such that the yaw axis pointed normal to the earth and the roll axis aligned with the spacecraft velocity vector, and which also maintained the solar paddles' orientation to the sun. The system permitted fine control of ± 1° in pitch and ± 0.5° in roll and yaw.

3.4 Source of Platform Mission Objectives

The Nimbus-5 mission had two major goals:

1. To help meet the objectives of NASA's expanding meteorological program (in 1972, the Nimbus-5 played a central role in this program).
2. To initiate satellite studies in the applications areas, particularly the development of advanced sensors for the exploration of natural resources and geophysical phenomena.

The meteorological program called for the application of space technology to increase understanding of the atmosphere and efficiency in making global meteorological observations. The Nimbus-5 provided a versatile orbital platform for a variety of experiments designed to:

- Observe atmospheric conditions and processes that influenced weather prediction
- Develop techniques for measuring global parameters required for modeling of atmospheric circulation.

3.5 Sensor or Instrument Description

ESMR consisted of four major components:

- A phased array microwave antenna consisting of 103 waveguide elements each having its associated electrical phase shifter. The aperture area is 83.3 cm X 85.5 cm. The polarization is linear, parallel to the spacecraft velocity vector.
- A beam steering computer that determines the coil current for each of the phase shifters for each beam position.
- A microwave receiver with a center frequency of 19.35 GHz and an IF bandpass of from 5 to 125 MHz; thus it is sensitive to radiation from 19.225 to 19.475 GHz, except for a 10 MHz gap in the center of the band.
- Timing, control and power circuits.

3.5.1 Principles of Operation

Unlike conical scan instruments such as the SMMR and SSM/I, the ESMR was a cross-scan instrument, with a resolution of approximately 30 km, which measured primarily the intensity of electromagnetic radiation thermally emitted from the Earth's surface at a wavelength of 1.55 cm (19.35 GHz). The instrument recorded radiation from 78 scan positions, and all observations were first converted to equivalent nadir observations.

3.5.2 Sensor/Instrument Measurement Geometry

The Nimbus-5 ESMR recorded radiation from 78 scan positions varying ± 50° from the satellite track every four seconds (Wilheit 1972). The beam width is 1.4° x 1.4° near nadir and degrades to 2.2° crosstrack x 1.4° downtrack at the 50° extremes. For a nominal orbit of 1100 km altitude, the resolution is 25 km x 25 km near nadir, degrading to 160 km crosstrack x 45 km downtrack at the ends of the scan. Full coverage of the entire polar area could be obtained from a sequence of six satellite orbits, or one-half day of good data, if all 78 beam positions were used; however, because of the large disparity in the radiometer field of view from the outer beam position to the middle beam position (70 km x 140 km compared with 25 km x 25 km), only the middle 52 beam positions were used for a swath-angle coverage of ± 30.5° and a minimum resolution of 29 km by 42 km. This swath angle corresponds to a spatial coverage of about 1280 km on the Earth's surface.

3.5.3 Calibration

The radiometer was originally calibrated using hot and cold reference sources. A sky horn measuring the 3 K cosmic background provided the cold-load temperature reference (Tc). The hot-load temperature was provided by reference to a floating ambient termination in the spacecraft. Calibration parameters are gathered from eight scans of data. Calibration temperatures (T_C and T_H) were calculated from multiplex data, and values of four ambient and four cold calibration voltages averaged through the set of eight scans. For each beam position the brightness temperature (Tin) corresponding to voltage (V) was then calculated by:

$$T_{IN} = TH + \frac{T_C - T_H}{V_C - V_H}(V - V_H)$$

3.5.4 Additional Calibration

A new calibration procedure was implemented in 1999 for the Nimbus-5 ESMR data at the same time the data were regridded from the orbital radiance data tapes to the polar stereographic grid. The new procedure included the removal of instrument drift and sensitivity jumps.

Studies of temporal brightness temperature variations in the Southern Ocean revealed some unexpected shifts. Because ocean brightness temperatures are expected to have minimal or no seasonal dependence, it was concluded that these could be caused only by calibration or instrument problems. Although brightness temperatures are affected by surface roughness, foam cover, water vapor, and rainfall, none of these have seasonal characteristics. Comiso and Zwally (1980) discuss the procedures used to normalize the data in response to these anomalous shifts.

While regridding orbital data to the polar stereographic grid, unusually high radiances resulting from instrument malfunction were omitted by gridding only values `0 < Tb < 310 K` in the Arctic and `0 < Tb < 282 K` in the Antarctic. Only the center 52 sets of values (center beam positions) were used, and 13 sets of values at the beginning and end of each data record were ignored; thus, no data are available poleward of approximately 86° latitude.

Instrumental drifts and meanders were adjusted by considering individual histograms of the radiances for each day. The typical histogram has two peaks in its distribution, one for open water and continental ice sheets and another for sea ice and land. The working premise is that the low-radiance wing of the ocean/ice sheet peak and the high-radiance wing of the sea ice/land peak are invariants except for seasonal changes. The seasonal swing on the high radiance end is from about 255 K - 285 K. At the low radiance end, it is about 120 K - 130 K. Multiple linear regression of all data was used to establish a nominal value of the presumed invariant radiance spread between these two wings. All single-day radiances were then adjusted by an automated procedure so that their histogram patterns match the nominal one in its spread.

North and south polar data were treated separately. The automated procedure entailed ascertaining the offset, slope and first five harmonics (ten trigonometric terms) of the annual cycle in the time series of fixed points (with outliers removed) in the threshold of the water/ice sheet distribution and the tail of the sea ice/land distribution. Models of the low and high radiance time series were constructed using the offset and ten trigonometric terms but not the slope, which was deemed to be an instrument drift. After applying the equations below, the remaining instrument drift was less than 0.1 K over the four-year period.

All radiances in each daily grid were then adjusted with the linear transformation:

```
Tbadjusted = a + b * Tboriginal
```

Where:

```
b = (Tbmodelmax - Tbmodelmin)/(Tbdatamax - Tbdatamin)
a = Tbmodelmin - (b * Tbdatamin)
```

`Tbmodelmax` is the daily value of the modeled high radiance wing point, and `Tbmodelmin` is the daily value of the modeled low radiance wing point. `Tbdatamax` is the daily value of the actual data high radiance wing point, and `Tbdatamin` is the daily value of the actual data low radiance wing point. When the actual data are near the model values, there is very little correction. The daily adjusted data were then visually inspected and any remaining unsuitable data were discarded. Unsuitable data were regarded as radiances that did not fit the above model.

Further corrections to the calibration were necessary to account for the antenna ohmic loss, which is a function of beam position and the temperature of the phase shifters, and for the effects of side lobes and the different viewing angles. A set of correction parameters for each beam position was empirically determined using ocean data and used to determine the final calibrated brightness temperatures.

Figures 3 and 4 are images of the ESMR brightness temperatures before and after the data adjustment.

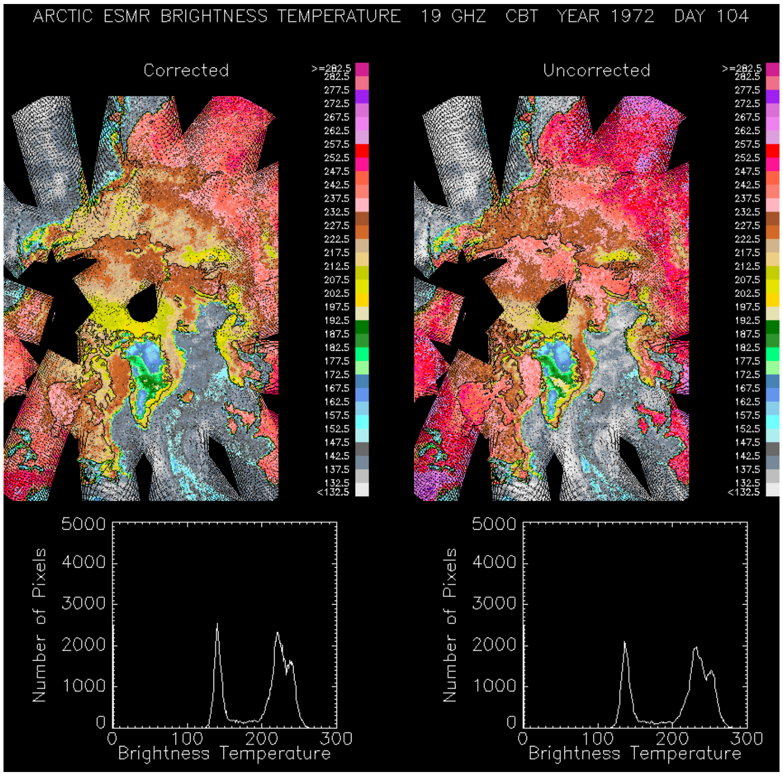

Figure 3. Arctic Day 104

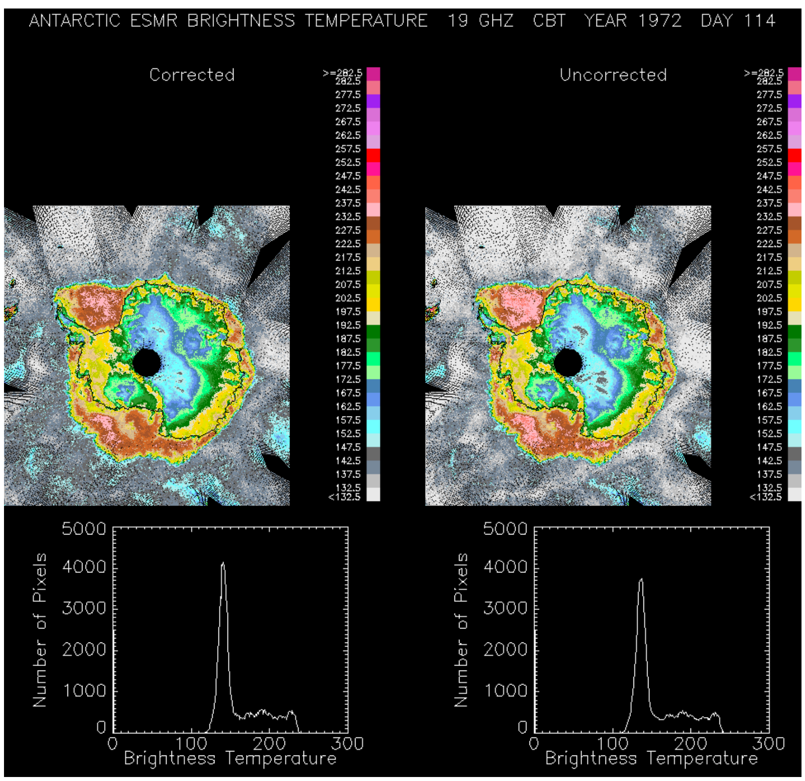

Figure 4. Antarctic Day 114

The original, uncorrected data files are available by special request from NSIDC User Services.

3.6 Data Source

The primary source of orbital Earth-located and calibrated radiometer data is the set of CBT tapes. The CBT tapes contain the time, calibration parameters, measured brightness temperatures, and corresponding geographical coordinates (Wilheit 1972). To provide synoptic representation of the data in the polar regions for both spatial and temporal studies, the orbital data were projected to polar stereographic maps and accumulated at fixed time intervals.

4 REFERENCES AND RELATED PUBLICATIONS

Comiso, J. C., and H. J. Zwally. 1980. *Corrections for Anomalous Time Dependent Shifts in Brightness Temperature from Nimbus-5 ESMR*. NASA TM-82055. Greenbelt, MD.

Parkinson, C., J. Comiso, H. J. Zwally, D. Cavalieri, P. Gloersen, and W. Campbell. 1987. *Arctic Sea Ice, 1973-1976: Satellite Passive-Microwave Observations.* NASA SP-489.

Parkinson, C., J. Comiso, and H. J. Zwally. 1987. *Satellite-Derived Ice Data Sets No. 2: Arctic Monthly Average Microwave Brightness Temperatures and Sea Ice Concentrations, 1973-1976*. NASA Technical Memorandum 87825.

Pearson, F. 1990. Map Projections: Theory and Applications. CRC Press. Boca Raton, Florida. 372 pages.

Snyder, J. P. 1987. Map Projections - A Working Manual. U.S. Geological Survey Professional Paper 1395. U.S. Government Printing Office. Washington, D.C. 383 pages.

Snyder, J. P. 1982. *Map Projections Used by the U.S. Geological Survey.* U.S. Geological Survey Bulletin 1532.

Wilheit, T. 1972. The Electrically Scanning Microwave Radiometer (ESMR) Experiment. *Nimbus-5 User's Guide*. NASA/Goddard Space Flight Center. p. 59-105.

Zwally, H. J., J. Comiso, C. Parkinson, W. Campbell, F. Carsey, and P. Gloersen. 1983. *Antarctic Sea Ice, 1973-1976: Satellite Passive-Microwave Observations*. NASA SP-459.

Zwally, H. J., J. Comiso, and C. Parkinson. 1981. *Satellite-Derived Ice Data Sets No. 1: Antarctic Monthly Average Microwave Brightness Temperatures and Sea Ice Concentrations 1973-1976*. NASA Technical Memorandum 83812.

4.1 Related Data Collections

- Nimbus-5 ESMR Polar Gridded Sea Ice Concentrations
- DMSP SSM/I-SSMIS Daily Polar Gridded Brightness Temperatures
- Nimbus-7 SMMR Polar Gridded Radiances and Sea Ice Concentrations
- NOAA/NASA Pathfinder Program SSM/I EASE-Grid Brightness Temperatures
- Sea Ice Concentrations from Nimbus-7 SMMR and DMSP SSM/I Passive Microwave Data

5 CONTACTS AND ACKNOWLEDGMENTS

Claire L. Parkinson, Joey C. Comiso, and H. Jay Zwally

NASA Goddard Space Flight Center Greenbelt, MD, USA

6 DOCUMENT INFORMATION

6.1 Publication Date

August 1999

6.2 Date Last Updated

May 2008